Article

Impact of Ocean Acidification on Energy Metabolism of Oyster, *Crassostrea gigas*—Changes in Metabolic Pathways and Thermal Response

Gisela Lannig [1],*, Silke Eilers [1], Hans O. Pörtner [1], Inna M. Sokolova [2] and Christian Bock [1]

[1] Alfred Wegener Institute for Polar and Marine Research in the Hermann von Helmholtz Association of National Research Centres e.V. (HGF), Am Handelshafen 12, 27570 Bremerhaven, Germany; E-Mails: Silke.Eilers@gmx.net (S.E.); Hans.Poertner@awi.de (H.O.P.); Christian.Bock@awi.de (C.B.)

[2] Department of Biology, University of North Carolina at Charlotte, 9201 University City Blvd., Charlotte NC, 28223, USA; E-Mail: ISokolov@uncc.edu (I.M.S.)

* Author to whom correspondence should be addressed; E-Mail: Gisela.Lannig@awi.de; Tel.: +49-(0)471-4831-2015; Fax: +49-(0)471-4831-1129.

Abstract: Climate change with increasing temperature and ocean acidification (OA) poses risks for marine ecosystems. According to Pörtner and Farrell [1], synergistic effects of elevated temperature and CO_2-induced OA on energy metabolism will narrow the thermal tolerance window of marine ectothermal animals. To test this hypothesis, we investigated the effect of an acute temperature rise on energy metabolism of the oyster, *Crassostrea gigas* chronically exposed to elevated CO_2 levels (partial pressure of CO_2 in the seawater ~0.15 kPa, seawater pH ~ 7.7). Within one month of incubation at elevated PCO$_2$ and 15 °C hemolymph pH fell (pH$_e$ = 7.1 $\pm$ 0.2 (CO_2-group) *vs.* 7.6 $\pm$ 0.1 (control)) and P_eCO$_2$ values in hemolymph increased (0.5 $\pm$ 0.2 kPa (CO_2-group) *vs.* 0.2 $\pm$ 0.04 kPa (control)). Slightly but significantly elevated bicarbonate concentrations in the hemolymph of CO_2-incubated oysters ([HCO$^-_3$]$_e$ = 1.8 $\pm$ 0.3 mM (CO_2-group) *vs.* 1.3 $\pm$ 0.1 mM (control)) indicate only minimal regulation of extracellular acid-base status. At the acclimation temperature of 15 °C the OA-induced decrease in pH$_e$ did not lead to metabolic depression in oysters as standard metabolism rates (SMR) of CO_2-exposed oysters were similar to controls. Upon acute warming SMR rose in both groups, but displayed a stronger increase in the CO_2-incubated group. Investigation in isolated gill cells revealed a similar temperature-dependence of respiration between groups. Furthermore, the fraction of cellular energy

demand for ion regulation via Na^+/K^+-ATPase was not affected by chronic hypercapnia or temperature. Metabolic profiling using ^{1}H-NMR spectroscopy revealed substantial changes in some tissues following OA exposure at 15 °C. In mantle tissue alanine and ATP levels decreased significantly whereas an increase in succinate levels was observed in gill tissue. These findings suggest shifts in metabolic pathways following OA-exposure. Our study confirms that OA affects energy metabolism in oysters and suggests that climate change may affect populations of sessile coastal invertebrates such as mollusks.

1. Introduction

Coastal zones are ecologically and economically important and are among those areas that will be strongly affected by global climate change. Increasing atmospheric CO_2 concentrations lead to increasing mean temperatures and a higher frequency of thermal extremes as well as to ocean acidification (OA). These environmental changes pose risks for marine ectothermal organisms that are not yet fully understood [2–4]. Current ecosystem changes are largely driven by temperature, whereas ecosystem impacts of elevated CO_2 are expected, but still have to be demonstrated for moderate oceanic PCO$_2$ levels that are predicted to occur over the next 100 years. Previous studies indicate that OA, "global warming's evil twin" (Richard Feely cited by [5]) will have mainly adverse consequences for many calcifying and non-calcifying organisms, and may result in changes to biodiversity, trophic interactions, and other ecosystem processes [4,6–11]. Marine organisms are affected by OA in several, mainly negative ways as shown by disturbances of acid-base regulation, respiration, energy turnover and metabolism, as well as a reduction in growth rates, reproductive success and calcification, and sensory abilities [12–20]. Depending on future CO_2 emission scenarios, predicted average surface seawater pH varies between 7.7 and 8.0 [21]. Deviation of environmental factors from the evolutionary optimum for a given species may result in deleterious impacts on energy homeostasis. Sub-optimal conditions create metabolic energy demands that may exceed energy supplied from food and/or accrued in somatic energy resources, as well as overwhelm the capacity of systemic functions (ventilation and circulation) and the cellular metabolic machinery to provide enough adenosine triphosphate (ATP) to sustain routine metabolism. An organism may compensate for elevated energy demand during the moderate stress by increasing energy intake and assimilation, and/or by elevated metabolic flux to cover ATP demand. However, during extreme stress exposures such compensation may be incomplete or impossible, and an organism can enter a metabolically depressed state to conserve energy and to extend the survival time until the conditions return to the optimum [22]. In either case, a disturbance of energy homeostasis will result in a limitation of aerobic scope of an organism, which in turn reduces the thermal tolerance limits of aquatic ectotherms [23]. Indeed, temperature-induced hypoxemia, transition to anaerobic energy production and oxidative stress were shown to play a critical role in determining the thermal tolerance limits and survival at elevated temperatures in aquatic ectotherms [24–29].

Recently, the concept of oxygen- and capacity-limited thermal tolerance of aquatic ectotherms [23] was extended to incorporate CO_2-driven effects predicting that the acute CO_2 stress will increase sensitivity of an organism to temperature change [1,4]. Indeed, hypercapnia caused a reduction in hemolymph O_2 partial pressure (P_eO_2) and narrowed the thermal tolerance window by a downward shift of the upper critical temperature in crabs, *Cancer pagurus* (1 kPa PCO_2, [30]) and *Hyas araneus* (0.3 kPa PCO_2, [31]). Michaelidis *et al.* [32] found no differences in P_eO_2 levels between control and hypercapnia-exposed mussels, *Mytilus galloprovincialis* (0.6 kPa PCO_2) when measured at the acclimation temperature. Following OA exposure extracellular pH (pH_e) dropped by 0.2 units and the standard metabolic rate (SMR) of the mussels decreased by about 60% indicating metabolic depression [32]. Metabolic depression acts as a time-limited adaptation strategy to survive unfavourable conditions such as hypercapnia [22]. Long-term performance and thus fitness is key to survival and success of a species. As summarized by Pörtner *et al.* [15], key physiological processes that are involved in setting the sensitivity to ocean acidification are the regulation of the organisms' cellular acid-base and ion status and the respective feed back loops on other processes that are associated with individual performance. Regulation of pH_e is thought to "be the first line of defense against hypercapnia induced disturbances of metabolic and tissue functioning" (p. 210) emphasizing a key role of pH_e in metabolic depression [33].

In contrast to vertebrates, most invertebrates exhibit a low capacity for acid-base regulation such that the changes in acid-base and ion status may directly interfere with the organism's performance [3,15,34,35]. Thus, the impact of future CO_2 concentrations is expected to be strong in invertebrates that are weak acid-base regulators and are unable to compensate the OA-induced shift in extracellular pH. Among this group, calcifying organisms may be particularly vulnerable to OA, because in addition to the acid-base disturbances they can experience disturbances in biomineralization needed for production of $CaCO_3$ exo- and endoskeletons [32,36–39]. As shown by Gazeau *et al.* [40] and Ries *et al.* [41], acute exposure to OA impairs the calcification of benthic mollusks already at calcium carbonate saturation values above 1 suggesting a decrease by 25% and 10% in mussel and oyster calcification by the end of the century with predicted PCO_2 levels of ~740 ppmv. In the mussel *M. galloprovincialis* long-term hypercapnia (seawater pH 7.3, ~0.6 kPa PCO_2) caused a reduction in hemolymph pH which was partly compensated by increased $[HCO_3^-]_e$ [32]. The increase in bicarbonate levels was likely linked to shell dissolution as indicated by increased extracellular $[Ca^{2+}]$ [32]. The drop in pH_e from 7.55 to 7.36 correlated with a reduction in metabolic rate and was suggested to be responsible for the observed growth rate reduction [32]. In *Mytilus edulis* chronically exposed to various CO_2 concentrations (seawater pH ranged from 6.7 to 8.1) growth increments were reduced when seawater pH fell below 7.4 [42].

In contrast to the bivalves, hypercapnia (0.4–0.6 kPa PCO_2, seawater pH of 7.1–7.2) did not depress metabolic rate and growth performance in the cephalopod, *Sepia officinalis*. Extracellular acidosis was compensated for by the accumulation of bicarbonate to a larger degree than in the bivalves but compensation remained incomplete [43]. These data indicate that CO_2 responses and thus tolerance thresholds may vary between animals depending on taxonomic group, acclimation history and degree of the hypercapnic stress.

Oysters are a major group of calcifiers in estuaries and coastal zones that may be strongly affected by OA and climate change. Estuarine and coastal organisms are regularly exposed to variable

temperature and pH values in their environment and thus may be less sensitive to acidification and global warming than their open-ocean counterparts that live in more stable thermal and pH environments [42]. However, estuarine and coastal areas are likely impacted the most in terms of the degrees and rates of projected warming and seawater acidification trends. In combination with lower salinity and thus depressed $CaCO_3$ saturation state these trends may strongly affect ectothermic calcifiers such as oysters [44]. We hypothesized that chronic OA exposure will affect energy metabolism in oysters and will have negative consequences on their temperature tolerance. To test this hypothesis we determined the impact of long-term OA/hypercapnia on temperature-dependent metabolism by analyzing the acid-base and metabolic status of the Pacific oyster, *Crassostrea gigas* under conditions simulating a future scenario in which CO_2 levels stabilize at ~0.1 kPa PCO$_2$ and water pH decreases by ~0.5 units [45]. We show that OA exposure leads to a disturbance of acid-base status and changes in the steady-state levels of metabolic intermediates and induces an increase in basal maintenance costs at elevated temperatures. These disturbances of energy metabolism indicate that performance and survival of estuarine invertebrates can be affected by even moderate OA scenarios supporting the recommendation by Turley *et al.* [46].

2. Results and Discussion

During the first days of CO_2 incubation oysters *C. gigas* showed delayed behavioral defense responses (e.g., were slow to close or did not close their shells in response to a touch; data not shown). However, the behavioural responses normalized during long-term CO_2 exposure (up to 55 days), and only one oyster out of 23 animals died after 22 days of CO_2 exposure, which equals a 4.3% mortality rate. No mortality was observed in the control group. Chronic hypercapnia resulted in significant changes in hemolymph parameters of oysters (Table 1). CO_2-exposed oysters showed elevated P_eCO$_2$ accompanied by lower hemolymph pH (decrease in pH$_e$ by ~0.5 units) compared to controls. A small but significant increase in [HCO$^-_3$]$_e$ was also observed in oysters following chronic hypercapnia. Chronic hypercapnia also affected concentrations of [Na$^+$]$_e$, [K$^+$]$_e$ and [Ca^{2+}]$_e$ in oyster hemolymph (Table 1). Hemolymph oxygenation was slightly affected by long-term hypercapnia with an approximately 20% reduction in hemolymph PO$_2$ in CO_2-exposed oysters (Table II; unpaired t-test, P = 0.07). Long-term hypercapnia also affected the body condition index of oysters that decreased marginally by ~20%, from 3.5 ± 0.6 (control) to 2.7 ± 0.7 (CO_2-exposed group)(unpaired t-test, N = 5–6, P = 0.052).

The ^{1}H-NMR spectra of the different tissues showed clear and reproducible specific metabolic profiles. Most of the signals did not change significantly between control and CO_2 exposed oysters in the various tissues, whereas concentrations of some metabolic intermediates were strongly affected by long-term hypercapnia in mantle and gill tissue (Figures 1b, c). In comparison the metabolic profile of muscle tissue was unaffected (Figure 1a). A strong depletion in alanine and ATP levels and a slight (non-significant) decline in glycogen concentrations was found in the mantle of CO_2-exposed oysters (Figure 1b). In gills, succinate levels were significantly elevated in CO_2-exposed oysters compared to their control counterparts (Figure 1c). A significant increase in succinate concentrations was also found in hepatopancreas of CO_2-exposed oysters compared to controls (data not shown).

Table 1. Hemolymph parameters of oyster, *C. gigas* after long-term incubation at control (normocapnia, seawater $P\text{CO}_2 \sim 0.054$ kPa) and elevated CO_2-concentrations (hypercapnia, seawater $P\text{CO}_2 \sim 0.15$ kPa, 26 to 55 days) at 15 ℃.

Parameter/Group	Control	CO$_2$-incubation
pH_e	7.60 ±0.10	7.09 ±0.18*
$P_e\text{CO}_2$ (kPa)	0.15 ±0.04	0.54 ±0.19*
$P_e\text{O}_2$ (kPa)	11.44 ±3.67	9.43 ±2.29 °
$C_e\text{CO}_2$ (mM)	1.67 ±0.11	2.15 ±0.30*
HCO_3^- (mM)	1.28 ±0.11	1.78 ±0.29*
Ca^{2+} (mM)	7.2 ±0.6	6.2 ±0.1 °
Na^+ (mM)	445.4 ±16.0	422.3 ±7.4*
K^+ (mM)	11.9 ±0.8	13.0 ±0.9*

(pH_e: extracellular pH; $C_e\text{CO}_2$: total dissolved inorganic carbon content). Data are means ±SD with N = 7–16 (control) and N = 6–23 (CO$_2$-incubation). * indicates significant differences between control and CO$_2$-incubated oysters (unpaired t-test, P < 0.05). ° indicates marginally significant differences between control and CO$_2$-incubated oysters (unpaired t-test, P = 0.07).

Figure 1. Levels of tissue metabolites in (a) muscle, (b) mantle and (c) gills of control (normocapnia, seawater $P\text{CO}_2 \sim 0.054$ kPa) and CO$_2$-exposed (hypercapnia, seawater $P\text{CO}_2 \sim 0.15$ kPa) oysters, *C. gigas* after long-term incubation at 15 ℃.
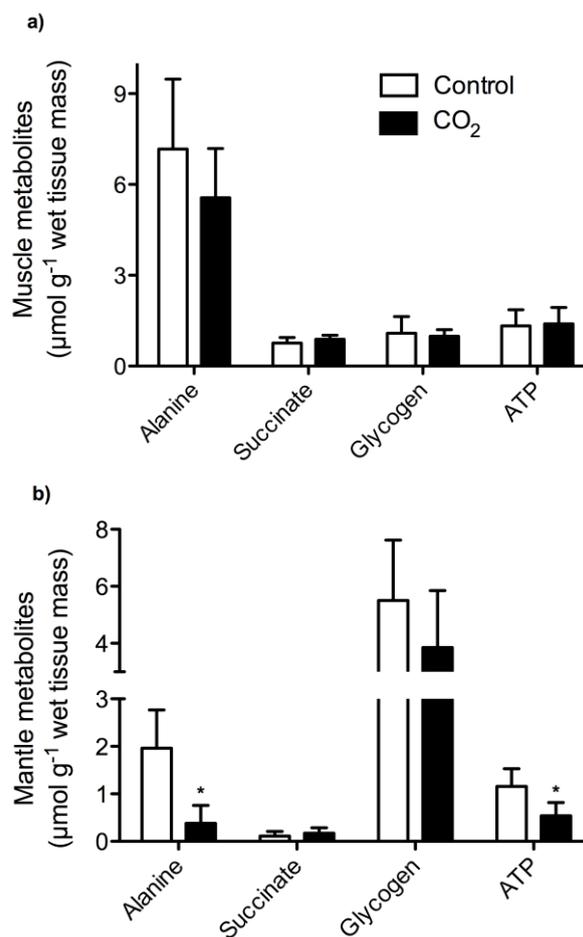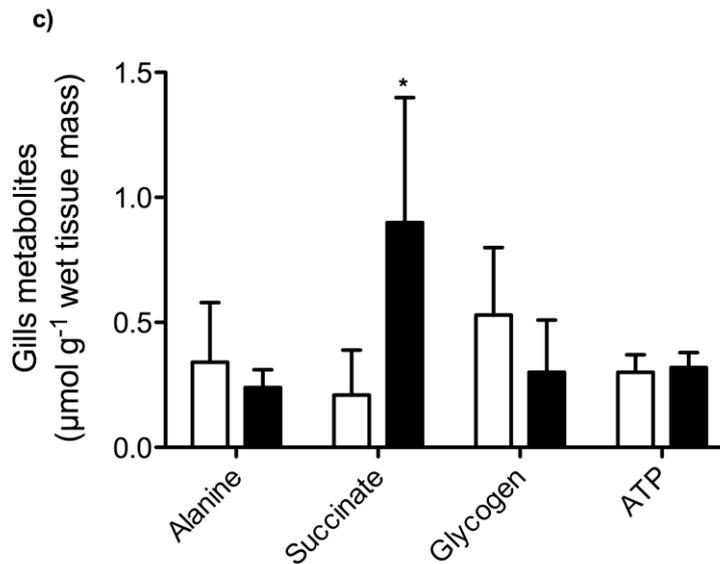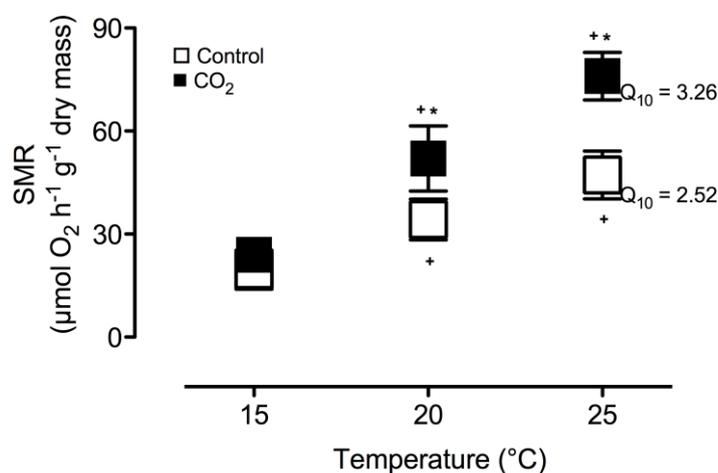
Figure 1. *Cont.*

Data are means ± SD with N = 6–8 (control) and N = 6–9 (CO_2-incubation). * indicates significant differences between control and CO_2-incubated animals (unpaired t-test, P < 0.05).

SMR was similar in control and CO_2-exposed animals when measured at the acclimation temperature of 15 °C (Figure 2). With warming SMR rose significantly in both groups revealing a stronger rise in SMR of CO_2-exposed compared to control animals as shown by higher Q_{10} values in the former group (Figure 2). As a result, SMR of CO_2-exposed oysters was significantly higher than in the controls at 20 °C and especially at 25 °C.
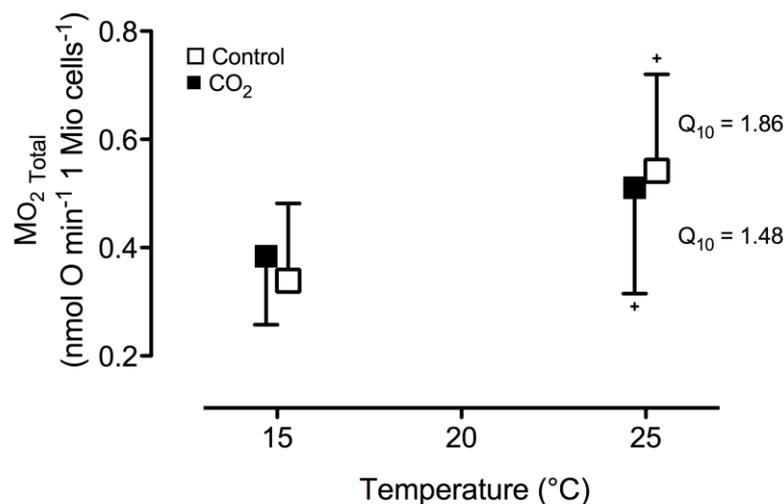
Figure 2. Normalized standard metabolic rate (SMR) in control (normocapnia, seawater PCO_2 ~ 0.054 kPa) and CO_2-exposed (hypercapnia, seawater PCO_2 ~ 0.15 kPa) oysters, *C. gigas* during acute warming (5 °C/48 h).

Data are means ± SD, N = 6 in each group. [+] indicates significant differences to the respective data at 15 °C (repeated measures ANOVA, P < 0.02). * indicates significant differences between control and CO_2-incubated animals at the respective temperature (unpaired t-test, P < 0.05). Differences in Q_{10} values between the groups were marginally significant (unpaired t-test, P = 0.06).

Contrary to whole animal SMR, we found no temperature-dependent effect of hypercapnia on respiration rates of isolated gill cells (Figure 3). Cellular respiration was significantly higher at 25 °C compared to 15 °C but the increase was similar in cells isolated from control and CO_2-exposed animals. Ouabain-sensitive respiration indicating energy demand for ion regulation via Na^+/K^+-ATPase comprised 33–37% of the total cellular oxygen demand and was not changed by temperature or by long-term hypercapnia ($P > 0.05$, data not shown).

Figure 3. Temperature-dependent respiration rates of isolated gill cells at the respective *in vivo* hemolymph pH of control (normocapnia, seawater $P\text{CO}_2$ ~ 0.054 kPa) and CO_2-exposed (hypercapnia, seawater $P\text{CO}_2$ ~ 0.15 kPa) oysters, *C. gigas* after long-term incubation at 15 °C.

Data are means ± SD with N = 6 (control) and N = 6–8 (CO_2-incubation). [+] indicates significant differences to respective data at 15 °C (paired t-test, P < 0.03). Q_{10} values did not differ significantly between the groups (unpaired t-test, P = 0.383).

Environmental change can be considered stressful if an organism needs to increase energy expenditure on maintenance, defense or repair. Stress-induced metabolic adjustments are aimed at reinstating the metabolic balance (*i.e.*, energy homeostasis) and thus ensuring survival of the individual and, most importantly, of the population. Energy homeostasis implies that the energy demand is covered by sufficient energy supply. Furthermore, there is a net energy gain to invest into production (somatic growth and reproduction). Therefore, any environmental disturbance that reduces this energy investment into production will have direct consequences for the organism's fitness.

Earlier studies in calcifying marine invertebrates including mollusks indicate that biomineralization is an energetically costly process. In molluskan shells consisting of inorganic crystals (calcite and/or aragonite) and an organic (mostly proteinaceous) matrix [72], production of the organic matrix was proposed to be the main cost-intensive process in shell growth [73]. Compared to the estimated total cost for inorganic shell material (1–2 J mg^{-1} $CaCO_3$), total costs for protein synthesis for shell formation are much higher (29 J mg^{-1}) and may explain the observed inverse relationship between rates of calcification and proportion of organic matrix in shells of marine mollusks [73,74]. However,

this is a conservative estimate of the cost of the inorganic shell material in mollusks because it does not take into account such energy-dependent aspects of calcification as the production of enzymes involved in calcium carbonate deposition (e.g., carbonic anhydrase), transport of $CaCO_3$ crystals by hemocytes and acid-base regulation at the site of $CaCO_3$ deposition [75–77]. Even with this conservative estimate, energetic costs for calcification could account for 75% of the total energy needed for somatic growth and may be up to four times higher than the amount of energy invested in reproduction, as shown in a rocky shore archeogastropod, *Tegula funebralis* [74]. After the shell is deposited, mollusks spend additional energy on its maintenance in order to counteract dissolution and erosion; in some intertidal limpets of the genus *Patella* the annual costs of shell erosion accounted for 8–20% of the total energy invested in production (somatic and shell growth and gonadal output)[78]. Such high energy expenditure for shell deposition and maintenance makes it likely that energetic trade-offs can also occur between shell, somatic growth and reproduction.

Exposure to elevated CO_2 levels and associated acidification of seawater can inhibit biomineralization rates and increase shell dissolution in marine mollusks [38,40,41,79] or as shown in some species of mollusks, crustaceans and echinoderms, calcification rates increased with decreasing seawater pH up to a certain point [41,51,80]. This may result in elevated metabolic costs of shell deposition and maintenance. The present investigation did not reveal an increase in basal metabolism in OA-exposed oysters when measured at acclimation temperature suggesting: (i) no OA-induced rise in costs or (ii) a shift in energy budget between tissues where a cost depression in one tissue is compensated for by the cost increment in another (see below). In the brittlestar *Amphiura filiformis* [80] the OA-induced increase in calcification rates coincided with an increase in respiration rates and was accompanied by a decrease in muscle mass [80]. The authors interpreted the loss in muscle mass as an energy source for the OA-induced elevated energy demands indicating a trade-off between structure (morphological integrity) and function (arm movement). In contrast, OA-exposed cephalopods *S. officinalis* gained soft body mass at similar rates as control animals although calcification rates were significantly higher in OA-exposed than in control animals [43]. In a following study the authors noted a reduced incorporation of organic matrix in the calcified structure of OA-exposed cephalopods [51] indicating again that a compensatory increase in calcification rates with increasing acidification comes at a cost.

Similar to previous reports on mussels [81] mild CO_2 accumulation according to OA scenarios had no impact on SMR of oysters at the acclimation temperature (15 ℃) indicating neither elevated energy demand nor metabolic rate depression in CO_2-exposed animals. However, SMR of CO_2-exposed animals was significantly above that of the normocapnic controls during acute warming indicating that hypercapnia resulted in elevated energy demand when combined with temperature stress. Moreover, the lowered condition index of CO_2-exposed animals suggested reduced growth efficiency due to a likely shift in energy budget in OA-exposed animals (see discussion above). Furthermore, it has been shown that hypercapnia interferes with protein turnover resulting in lowered protein synthesis in marine organisms [80,82,83], which may explain reduced growth under elevated CO_2 levels despite unchanged respiration rates.

Whole animal respiration rates gives an estimation of the overall sum of all energy consuming processes, making it likely to oversee small changes in specific processes or if the change in one process is compensated for by another. In line with observations cited above the rise in calcification

costs may compensate for metabolic depression in other tissues like muscle or gills such that a net effect of OA on SMR of the whole animal does not occur. In this context, OA-induced alterations in metabolite profiles of oyster gills and mantle indicate that hypercapnia has an impact on metabolic pathways in these tissues. In gills and hepatopancreas, the most notable alteration was an increase in succinate concentration during prolonged exposure to elevated CO_2 levels. Succinate accumulation is considered an indicator of anaerobic metabolism in bivalves including oysters [84,85]. Succinate accumulation in CO_2-exposed oysters in our study may only be due to a transition to partial anaerobiosis in the respective organs. We cannot exclude such oxygen limitation to set in as we found a small reduction in hemolymph oxygenation at constant SMR during long-term hypercapnia at 15 °C. This indicates that tissues may not become fully hypoxemic under these conditions but tissue-specific microperfusion may have been disturbed. However, further study is needed to corroborate our conclusions. In contrast to familiar patterns of anaerobic metabolism, no alanine accumulation was observed in gills or hepatopancreas (data for hepatopancreas not shown). Alanine is an early indicator of acute anaerobiosis in marine bivalves including oysters and its accumulation typically precedes that of succinate [84–86]. Hypercapnia also resulted in a strong (by ~80%) depletion of alanine levels in the mantle tissues of oysters. Given that osmotic and hypoxic stress, two major modulators of amino acid levels in bivalves, can be ruled out in our study, the drop in alanine levels of mantle tissue of OA exposed oysters may reflect increased gluconeogenesis. In fully aerobic cells this process may occur and compensate for the putative accumulation of alanine in anaerobic cells. An OA-induced shift in metabolic pathways favoring gluconeogenesis due to an OA-induced impairment of glycolysis was also suggested in fish [87]. We suggest that alanine is transaminated to pyruvate, which together with ATP will be used to build up phosphoenolpyruvate (PEP), with PEP as substrate entering the gluco-neogenetic pathway. The glucose synthesized from alanine in the mantle can then be used to fuel the metabolic demand of mantle and most likely transported to other tissues like the gills. However, a non-significant trend (due to the high variability between individuals) for a decrease in the glycogen level was observed in the mantle tissue of hypercapnic oysters, which would be consistent with elevated glycolytic flux. Hypoxemia may prevent enhanced gluconeogenesis to be effective in replenishing glycogen levels. Further investigations are needed to determine activities of enzymes involved in glycolysis and gluconeogenesis and/or metabolite fluxes in different tissues to fully unravel the mechanisms of the observed metabolite shifts and their physiological consequences at the whole-organism level.

Extracellular pH has been identified as an important determinant of metabolic rate of muscle tissue and (vertebrate) liver, and metabolic rate can drop if pH_e decreases below a certain threshold level [33]. OA exposure caused a marked acidosis in extracellular fluids of *C. gigas*, which remained largely uncompensated as bicarbonate levels increased only slightly. Along with the relative stability of bicarbonate levels, extracellular $[Ca^{2+}]$ also did not change during hypercapnia in *C. gigas* indicating no dissolution of shell or tissue calcium carbonate. In contrast, hypercapnia-induced acidification of seawater (pH = 7.3) resulted in a decrease of pH_e in *M. galloprovincialis* and a significant increase in hemolymph Ca^{2+} levels which was interpreted as partial buffering of pH_e by shell dissolution [32]. Our findings are in line with recent studies in blue mussels *M. edulis* and the Greenland smoothcockle, *Serripes groenlandicus*, where no significant change in extracellular $[HCO_3^-]$ and $[Ca^{2+}]$ was noted with increasing seawater P_{CO_2} up to 0.4 kPa [88–90]. Possibly, the degree of involvement of the shell

and tissue $CaCO_3$ in buffering of the hemolymph pH depends on the degree of acidification and may become notable when the environmental pH decreases below a certain species-specific threshold. Furthermore, as discussed by Hardewig *et al.* [91] "metabolism itself may contribute to the regulation of acid-base balance". Pörtner [92] suggested that PEP can be carboxylated under hypercapnia resulting in an increase of succinate (as observed in this study) and propionate concentrations accompanied with the consumption of bicarbonate or CO_2, an additional benefit under hypercapnic conditions [88].

Concomitant with the more acidic pH_e, Michaelidis *et al.* [32] found reduced respiration rates in OA-exposed mussels. Also in oysters (*C. virginica*), Willson and Burnett [69] reported a lowered oxygen uptake in animals subjected to high CO_2 partial pressures: high (0.8–1 kPa PCO_2, seawater pH ≤ 7) compared to controls at low (<0.1 kPa PCO_2, seawater pH 8.2). In line with findings at the whole animal level, oxygen uptake of isolated gill tissue from oysters, *C. virginica* was depressed under the low pH conditions irrespective of the CO_2 levels [69]. Reipschläger and Pörtner [68] and Pörtner *et al.* [93] provided conclusive evidence that and how metabolic depression in isolated body wall musculature of the peanut worm *Sipinculus nudus* under hypercapnia was specifically due to lowered extracellular pH rather than intracellular pH, elevated PCO_2 or modified bicarbonate levels. In our experiments, seawater pH fell to 7.7 and no pH_e compensation was observed (pH_e = 7.1). At the temperatures tested CO_2-exposed animals showed no sign of metabolic depression and, similarily, isolated gill cells showed no change in respiration rates when measured in buffer that was adjusted to the respective pH_e [7.6 (control) *vs.* 7.1 (CO_2-group)]. Different temperature sensitivities suggest, however, that upon cooling, CO_2 may cause metabolic rate to fall below controls. Our findings suggest that within the tested temperature range the pH_e reached during exposure to mild hypercapnia as in this study is found above the threshold triggering overall metabolic rate depression in *C. gigas*.

Ion regulation capacity via Na^+K^+-ATPase showed no difference between gill cells isolated from control and CO_2-exposed animals. The data for Na^+K^+-ATPase regulation under hypercapnia are sparse and contradictory suggesting species-specific thresholds in CO_2-induced impact on Na^+K^+-ATPase capacity. Thus, in some species elevated CO_2 levels have no effect on activity of Na^+K^+-ATPase (2 kPa PCO_2, [94]) whereas in others increased Na^+K^+-ATPase activity was observed after acclimation to long-term hypercapnia (1–5 kPa PCO_2, [17,95]). Melzner *et al.* [3] observed a concentration-dependent effect of CO_2 on Na^+K^+-ATPase activity in cod gills with unchanged activity at 0.3 kPa PCO_2, and increased activity at 0.6 kPa PCO_2. In *S. nudus*, extracellular pH modulates the energy costs for acid-base regulation by a shift from less to more ATP-efficient ion transporters during hypercapnia resulting in a reduction of Na^+K^+-ATPase activity due to reduced requirement for sodium regulation [68,93,96]. In CO_2-exposed oysters the observed lowering of extracellular $[Na^+]$ and elevation of $[K^+]$ compared to controls is consistent with the hypothesized shift to more ATP-efficient ion transporters. If it holds true in oysters, the associated changes in Na^+K^+-ATPase activity must be small and undetectable by the method employed in our present study (determination of ouabain-sensitive respiration). To date, many different ion transporters have been identified [97,98] but the complex interplay of these proteins regulation ion- and pH balance is not yet fully understood and requires further investigation.

3. Experimental Section

3.1. Animal collection and maintenance

Wild adult oysters, *Crassostrea gigas* (80 to 130 mm shell length) were collected at the North Sea coast near the islands of Langeoog and Baltrum (catch position: 53°42' North, 7°26' East) in March 2009. Salinity was ~29 psu and water temperature ~7 ℃ at the time of collection. Animals were covered with wet towels in polystyrene boxes at 8–12 ℃ and transported to the Alfred Wegener Institute (Bremerhaven, Germany) within 24 h of collection. Oysters were separated from each other, washed and cleaned from epibionts and maintained in recirculating aerated water tanks with filtered natural seawater from the North Sea at 15 $\pm$1 ℃ and 32 $\pm$1 psu. Following pre-acclimation for at least 30 days, during which no mortality occurred, oysters were randomly divided into a control group and a CO_2-exposed group with two to three replicate tanks per group. Animal density in the tanks was maintained at one oyster per 6 L of seawater. Oysters were fed three times a week *ad libitum* with a commercial algal blend containing *Nannochloropsis*, *Phaeodactylum tricornutum* and *Chlorella* (DT's Live Marine Plankton, Coralsands, Germany, www.coralsands.de).

For CO_2 incubations, elevated PCO_2 was produced by gas mixtures of 99.9% CO_2-free air and 0.1% CO_2 gas using Wösthoff gas mixing pumps (Wösthoff GmbH, Germany, http://www.woesthoff.com). All animal tanks (experimental, incubation and reservoir tanks for water changes) were continuously bubbled with the ambient air or air-CO_2 mixtures as appropriate, and water change was performed every other day to ensure adequate water quality. Parameters were measured in water samples at least three times a week immediately before and 1 to 2 h after a water change (see Table 2).

Table 2. Physicochemical conditions of seawater during control (normocapnia) and CO_2-incubation (hypercapnia) of oyster, *C. gigas* at 15 ℃.

Parameter/Group	Control	CO_2-incubation
Salinity (psu)	32.1 $\pm$0.5	31.3 $\pm$0.4
pH $_{NBS}$	8.07 $\pm$0.04	7.68 $\pm$0.07
PCO_2 (kPa)	0.059 $\pm$0.008	0.15 $\pm$0.026
$[HCO_3^-]$ (mmol kg^{-1})	2.09 $\pm$0.09	2.24 $\pm$0.12
Ω Ar	2.31 $\pm$0.30	0.87 $\pm$0.15
Ω Ca	3.59 $\pm$0.44	1.36 $\pm$0.24

NBS: National Bureau of Standards; PCO_2: seawater partial pressure of CO_2; Ω Ar and Ca: saturation state of aragonite and calcite, respectively. Data are means $\pm$ SD with N = 11 (control) and N = 37 (CO_2-incubation).

Alkalinity was measured by potentiometric titration (METROHM Prozessanalytik GmbH&Co, Germany, see [47]). The CO_2 incubations lasted for 26–55 days and the physicochemical parameters of the seawater are reported in Table I. Parameters of carbonate chemistry were calculated from temperature, salinity, pH and total alkalinity of the seawater with the software CO2SYS [48] using the equilibrium constants of Mehrbach *et al.* [49] as refitted by Dickson and Millero [50–52].

3.2. Tissue and hemolymph collection

To minimize stress, oysters were taken out from the incubation tanks one at a time and put on ice for immediate processing. Hemolymph samples were taken anaerobically from the intact pericardium (no hemolymph samples were taken if pericardium was damaged) with gas-tight syringes and either measured immediately (for acid-base parameters and gas concentrations) or prepared for further analyses of ion concentrations. Tissue samples (gills, mantle, muscle, hepatopancreas) were taken, immediately freeze clamped and stored in liquid nitrogen for further analyses.

3.3. Determination of hemolymph acid-base parameters, P_eCO_2, P_eO_2 and C_eCO_2

Hemolymph parameters (pH$_e$, P_eCO_2 and P_eO_2) were measured immediately after sampling using a blood gas analyzing system (combined system with glass pH electrode, PCO_2 and PO_2 electrode) from Eschweiler (MT 33, Eschweiler, Germany). The instrument was calibrated at the respective acclimation temperature (15 ℃) and allows for accurate measurements at low gas concentrations. Total CO_2 concentration in hemolymph (C_eCO_2) was analyzed by gas chromatography (Agilent 6890N GC System, Agilent Technologies, USA, see 53). Apparent bicarbonate concentrations in the hemolymph ([HCO$^-_3$]$_e$) were calculated as follows:

$$[HCO^-_3]_e = C_eCO_2 - (\alpha CO_2 \times P_eCO_2)$$

where C_eCO_2 = total CO_2 concentration in hemolymph (mM), αCO_2 = solubility of CO_2 in hemolymph calculated after Heisler [54] (0.0525 mmol L^{-1} Torr^{-1}), and P_eCO_2 = partial pressure of CO_2 in hemolymph (Torr).

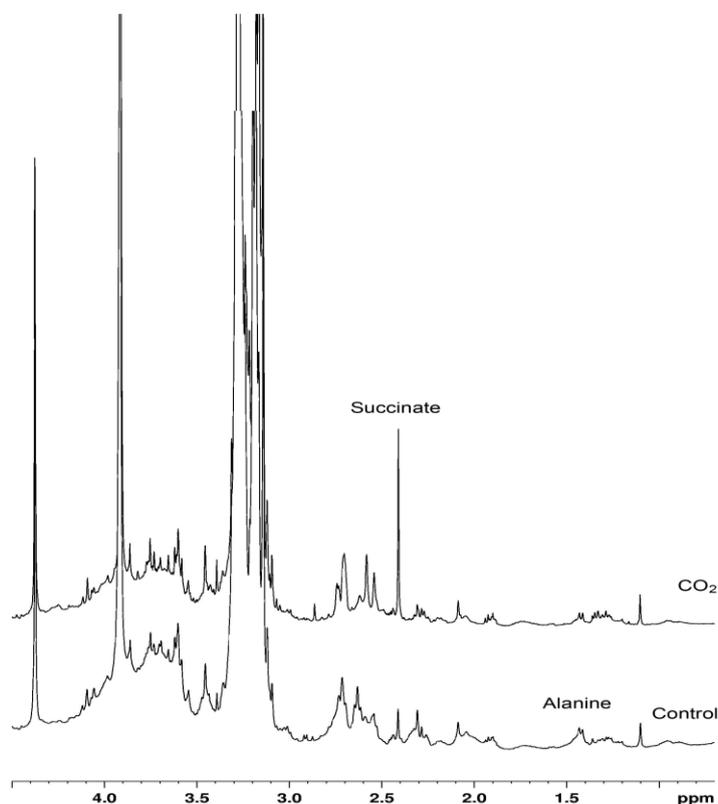For ion analysis (sodium [Na$^+$], potassium [K$^+$], magnesium [Mg^{2+}], calcium [Ca^{2+}] and ammonium [NH$_4^+$]), hemolymph samples were centrifuged (19,000 g, 20 min, RT) and plasma samples were stored at -80 ℃ for later measurements. Defrosted plasma samples were diluted 1:300 to 1:500 with deionised H$_2$O which yielded good signal to noise ratios, and ion concentrations were measured via ion chromatography (ICS-2000, Dionex®, Germany, see [55]).

3.4. Determination of metabolites

For the determination of metabolite concentrations in muscle, mantle and gill tissues, frozen tissue samples were powdered with mortar and pestle under liquid nitrogen. Tissue powder (~0.3 g) was added to an excess (5×) volume of ice-cold 0.6 M perchloric acid (PCA) and homogenized by ultrasonic treatment (0 ℃, 360 Watt). Precipitated protein was removed by centrifugation (0 ℃, 2 min at 16,000 g). The supernatant was neutralized with 5 M potassium hydroxide (KOH) to pH 7.0–7.5. Precipitated potassium perchloride was removed by a second centrifugation (0 ℃, 2 min at 16,000 g). Extracts were stored at -80 ℃ for further analyses. For NMR spectroscopy, samples were freeze-dried by centrifugation in a SpeedVac. Dried samples were diluted in D$_2$O (resulting in a final concentration of 0.3 g initial tissue powder per mL), mixed and transferred to 5 mm NMR tubes. Fully relaxed one-dimensional (1D), one pulse ^{1}H-NMR spectra of tissue extracts were recorded with an inversed ^{1}H-broad band probe (^{1}H/BBI) using a 9.4 T Avance 400 WB spectrometer (Bruker Biospin GmbH, Germany). Parameters were as follows: flip angle 90 °, spectral width 4k, time domain 16k, acquisition

time 2.04 s, relaxation delay 12 s, 64 scans (+2 dummy scans), resulting in a scan time of 15.3 min. Spectra were processed and analyzed using TopSpin 2.5 (Bruker Biospin GmbH, Germany). Prior to Fourier transformation all data were zero filled to 64k and processed with an exponential multiplication of 0.5 Hz. After phase and baseline correction, spectra were calibrated to TMS (at 0.0 ppm) that was added to the tissue extracts. Specific metabolites were identified using chemical shift tables [56–62]. Following signals were identified in the different tissues: formate, histidine, phenylalanine, tryptophan, ATP, glycogen, glycine-betaine, betaine/TMAO, choline, arginine, aspartate, ketoglutarate, succinate, glutamine, GABA, acetate, alanine, propanediol. Metabolites of interest such as succinate/alanine were analysed in more detail (see Figure 4 and the result part). Metabolite concentrations were determined by integration of NMR signals using the integration routine in TopSpin. All integrals were calibrated to the integral of a 1mM succinate solution that was determined in a separate standard sample using the same acquisition parameters as for our tissue samples.

> **Figure 4.** Example of ^{1}H-NMR spectra from gill tissue extracts of control and CO$_2$-exposed oysters. A clear increase in succinate can be observed following hypercapnia.

3.5. Determination of standard metabolic rate and animal condition index

SMR was measured as resting oxygen consumption in control and CO$_2$-exposed oysters using microfiber optic oxygen probes (Tx-Type, PreSens GmbH, Germany, http://www.presens.de)[63]. To avoid interference with postprandial metabolism and feces excretion, animals were fasted for 24 h

prior to the start of SMR recordings. Two-point calibration (N_2-bubbled seawater for 0% and air-bubbled seawater for 100% air saturation) was performed at each temperature (15, 20 and 25 °C). The oxygen consumption rate was first measured at the acclimation temperature of 15 °C, then the temperature was increased to 20 °C overnight and oxygen consumption measured the following day. After 48h the temperature was increased again by 5 °C overnight and the final determination of oxygen consumption was conducted at 25 °C. After measurements, oysters were dissected and tissue dry mass was determined. SMR was calculated as follows:

$$SMR = (\Delta PO_2 \times \beta O_2 \times Vfl)/M^{0.8}$$

where SMR is the oxygen consumption normalized to 1 g dry tissue mass ($\mu molO_2$ g^{-1} dry mass h^{-1}), ΔPO_2 the difference in partial pressure between in- and out-flowing water (kPa), βO_2 the oxygen capacity of water ($\mu molO_2$ L^{-1} kPa^{-1}), Vfl the flow rate (L h^{-1}), M the oyster tissue dry mass (g) and 0.8 is the allometric coefficient for *C. gigas* [64].

A general condition index (CI) of the experimental oysters was calculated as follows [63,65,66]:

$$CI = tissue\ dry\ mass\ (g)/shell\ dry\ mass\ (g) \times 100$$

3.6. Determination of cellular respiration rates and fractional cost for ion regulation via Na^+/K^+ ATPase

Cells were isolated from gills of control and CO_2-exposed oysters using a protocol modified from Cherkasov *et al.* [67]. Gills from 2–3 oysters were pooled, minced and washed twice in ice-cold buffer A (in mM: NaCl 423, KCl 9.1, $CaCl_2$ 9.3, $NaHCO_3$ 2.1, Hepes 30 at pH 7.5 or 7.1 for cell isolation from control or CO_2-incubated oysters, respectively). The tissue was digested with 0.125% Trypsin/EDTA in balanced Hank's solution adjusted to 720 mOsm with sucrose. Dissected gills were gently shaken in the digestion solution for ~30 min at room temperature (0.5 g tissue mL^{-1} solution). Digestion was stopped by adding 5–10% (v:v) fetal calf serum. The extract was filtered through 100 μm sterile nylon mesh, washed twice with buffer A and centrifuged for 10 min at 400g and 4 °C to pellet the cells. Cell pellets were washed three times in buffer A, combined and finally resuspended in buffer B (in mM: NaCl 423, KCl 9.1, $CaCl_2$ 9.3, $NaHCO_3$ 2.1, $MgCl_2$ 22.9, $MgSO_4$ 25.5, glucose 15, Hepes 30 at pH 7.5 or 7.1 for cell isolation from control or CO_2-incubated oysters, respectively). In the pilot experiments, we measured cellular respiration using buffer B adjusted for pH and PCO_2 to mimic the hemolymph parameters of control and CO_2-exposed oysters, respectively. The elevated pCO_2 of the buffer had no effect on cell respiration (data not shown) which agrees with the results of previous studies [68,69]; therefore, in the subsequent experiments, only pH was adjusted to simplify the experimental logistics.

Cell density was determined in a Fuchs–Rosenthal counting chamber and adjusted to 10×10^6 cells mL^{-1}. Cell viability was assessed by using a standard Trypan Blue exclusion assay and was found to be >80%. Cellular respiration was determined in 1 mL water-jacketed, air-tight chambers using microfiber optic oxygen probes (Tx-Type, PreSens GmbH, Germany, http://www.presens.de). A two-point calibration was performed at each temperature (15 and 25 °C) using saturated sodium sulfide solution for 0% and air-bubbled medium for 100% air saturation. Cellular oxygen consumption in the absence of inhibitors ($MO_{2\ total}$), and MO_2 in the presence of 1mM and 10mM ouabain to inhibit

Na$^+$/K$^+$-ATPase were recorded (MO$_{2\,\text{ouabain}}$, both concentrations showed a similar degree of inhibition of cellular MO$_2$ and, thus, were counted as replicates)[70,71]. Cell respiration rates were calculated as follows:

$$\text{MO}_2 \ (\text{nmol O min}^{-1} \ 10^6 \ \text{cells}^{-1}) = -m \times (P\text{O}_2/100\%) \times \text{ß}\text{O}_2 \times \text{V}_{\text{cell}}/\text{N}$$

where m is the slope of the decrease of oxygen saturation in the respiration chamber (% min^{-1}), $P\text{O}_2$ is the oxygen partial pressure at 100% saturation (Torr), $\text{ß}\text{O}_2$ is the oxygen capacity of the solution (μmol O$_2$ L^{-1} Torr^{-1}), V$_{\text{cell}}$ is the volume of the cell suspension used (L), and N is the number of cells in the V$_{\text{cell}}$ of cell suspension.

Oxygen demand for ion regulation via Na$^+$/K$^+$-ATPase was calculated as follows:

$$\text{MO}_{2\text{NaK ATPase}} \ (\text{nmol O min}^{-1} \ 10^6 \ \text{cells}^{-1}) = \text{MO}_{2\,\text{total}} - \text{MO}_{2\text{ouabain}}$$

Prior to oxygen consumption measurements 0.5–1 mL of cell suspension was centrifuged and 2/3 of the supernatant was exchanged by fresh buffer B to ensure saturated oxygen and substrate concentration for maximal cell respiration. All chemicals and media were obtained from Sigma-Aldrich (Germany).

3.7. Statistical analysis

Statistical analyses were carried out using InStat 3.0b and Prism 5.0b (GraphPad Software, Inc.). Differences between measured parameters of control and CO$_2$-incubated animals were determined by unpaired t-test (parametric test) or Mann-Whitney test (non-parametric test) as appropriate depending on the normality of distribution of the dependent variable. Temperature effects on whole animal and cellular respiration rates were tested by repeated measures ANOVA and paired t-test, respectively. The differences were considered significant if P < 0.05 unless stated otherwise. All data are presented as mean values ± standard deviation (SD).

4. Conclusions

Our present study demonstrates that CO$_2$ levels corresponding to expected OA scenarios are likely to interfere with the energy metabolism of oysters. This may reflect vulnerability to OA and temperature extremes. These findings are especially noteworthy because oysters, like other estuarine invertebrates, are normally exposed to broad fluctuations in CO$_2$ levels, pH and temperature in their habitats and thus should be better adapted to these changes than their deep-water or open-ocean counterparts. Nevertheless, chronic hypercapnia affects energy metabolism even in this eurybiont species especially when combined with elevated temperature. Synergistic effects of elevated temperature and hypercapnia were also identified in other bivalves [89,99] and are consistent with earlier reports that elevated temperature enhanced the sensitivity to a variety of environmental stressors such as pollution, hypercapnia or oxygen deficiency [1,4,100]. However, species-specific physiological differences in biomineralization as well as energy metabolism and acid-base regulation may shape differential sensitivities of various marine invertebrates to OA and elevated temperature thus complicating the picture of ecosystem-level responses of marine organisms to a high CO$_2$ world. Further studies are critically needed to determine the range of sensitivities of key marine species to OA

and global climate change and the mechanisms setting limits to their tolerance to elevated temperatures and low pH in the future oceans. Analyses of energy metabolism as in the present study can provide a useful integrative view of stress effects on physiological performance of a variety of marine species and characterize their tolerance and tolerance limits in the face of global change.

Acknowledgements

References

1. Pörtner, H.O.; Farrell, A.P. Physiology and climate change. *Science* **2008**, *322*, 690–692.
2. Fabry, V.J. Marine calcifiers in a high-CO_2 ocean. *Science* **2008**, *320*, 1020–1022.
3. Melzner, F.; Göbel, S.; Langenbuch, M.; Gutowska, M.A.; Pörtner, H.O.; Lucassen, M. Swimming performance in Atlantic Cod (*Gadus morhua*) following long-term (4–12 months) acclimation to elevated seawater P_{CO_2}. *Aquat. Toxicol.* **2009**, *92*, 30–37.
4. Pörtner, H.O. Oxygen- and capacity-limitation of thermal tolerance: a matrix for integrating climate-related stressor effects in marine ecosystems. *J. Exp. Biol*. **2010**, *213*, 881–893.
5. Savitz, J.; Harrould-Kolieb, E. The oceans' acid test: can our reefs be saved? *Front. Ecol. Environ.* **2008**, *6*, 515.
6. Royal Society. Ocean acidification due to increasing atmospheric carbon dioxide. Policy Document 12/05. The Royal Society: London, UK, 2005.
7. Kleypas, J.A.; Feely, R.A.; Fabry, V.J.; Langdon, C.; Sabine, C.L.; Robbins, L.L. Impacts of ocean acidification on coral reefs and other marine calcifiers: a guide for future research. Report of a workshop held on 18–20 April 2005, St Petersburg, FL, USA, 2006.
8. Hall-Spencer, J.M.; Rodolfo-Metalpa, R.; Martin, S.; Ransome, E.; Fine, M.; Turner, S.M.; Rowley, S.J.; Tedesco, D.; Buia, M.C. Volcanic carbon dioxide vents show ecosystem effects of ocean acidification. *Nature* **2008**, *454*, 96–99.
9. Fabry, V.J.; Seibel, B.A.; Feely, R.A.; Orr, J.C. Impacts of ocean acidification on marine fauna and ecosystem processes. *ICES J. Mar. Sci.* **2008**, *65*, 414–432.
10. Andersson, A.J.; Mackenzie, F.T.; Bates, N.R. Life on the margin: Implications of ocean acidification on Mg-calcite, high latitude and cold water marine calcifiers. *Mar. Ecol. Prog. Ser.* **2008**, *373*, 265–273.

11. Reid, P.C.; Fischer, A.; Lewis-Brown, E.; Meredith, M.P.; Sparrow, M.; Andersson, A.J.; Antia, A.; Bathmann, U.; Beaugrand, G.; Brix, H.; *et al.* Impacts of the Oceans on Climate Change. *Adv. Mar. Biol.* **2009**, *56*, 1–150.

12. Riebesell, U.; Zondervan, I.; Rost, B., Tortell, P.D.; Zeebe, R.E.; Morel, F.M.M. Reduced calcification of marine plankton in response to increased atmospheric CO_2. *Nature* **2000**, *407*, 364–367.

13. Caldeira, K.; Wickett, M.E. Oceanography: anthropogenic carbon and ocean pH. *Nature* **2003**, *425*, 365.

14. Caldeira. K.; Wickett, M.E. Ocean model predictions of chemistry changes from carbon dioxide emissions to the atmosphere and ocean. *J. Geophys. Res.* **2005**, *110*, C09S04.

15. Pörtner, H.O.; Langenbuch, M.; Reipschläger, A. Biological impact of elevated CO_2 concentrations: lessons from animal physiology and earth history. *J. Ozenogr.* **2004**, *60*, 705–718.

16. Ishimatsu, A.T.; Kikkaea, T.; Hayashi, M.; Lee, K.S.; Kita, J. Effects of CO_2 on marine fish: larvae and adults. *J. Oceanogr.* **2004**, *60*, 731–741.

17. Ishimatsu, A.; Hayashi, M.; Lee, K.S.; Kikkawa, T.; Kita, J. Physiological effects on fishes in a high-CO_2 world. *J. Geophys. Res.* **2005**, *110*, doi:10.1029/2004JC002564.

18. Pörtner, H.O. Auswirkungen von CO_2-Eintrag und Temperaturerhöhung auf die marine Biosphäre. In *Die Zukunft der Meere – zu warm*, *zu hoch*, *zu sauer*; Schubert, R., Schellnhuber, H.J., Buchmann, N., Epiney, A., Grieshammer, R., Kulessa, M., Messner, D., Rahmstorf, S., Schmid, J., Eds.; Sondergutachten des WBGU: Berlin, Germany, 2006.

19. Green, M.A.; Waldbusser, G.G.; Reilly, S.L.; Emerson, K.; O'Donnella, S. Death by dissolution: sediment saturation state as a mortality factor for juvenile bivalves. *Limnol. Oceanogr.* **2009**, *54*, 1037–1047.

20. Munday, P.L.; Dixson, D.L.; Donelson, J.M.; Jones, G.P.; Pratchett, M.S.; Devitsina, G.V.; Doving, K.B. Ocean acidification impairs olfactory discrimination and homing ability of a marine fish. *Proc. Natl. Acad. Sci.* **2009**, *10*, 1848–1852.

21. Meehl, G.A.; Stocker, T.F.; Collins, W.D.; Friedlingstein, P.; Gaye, A.T.; Gregory, J.M.; Kitoh, A.; Knutti, R.; Murphy, J.M.; Noda, A.; *et al.* Global climate projections. In *Climate Change 2007: The Physical Science Basis. Contribution of Working Group I to the Fourth Assessment Report of the Intergovernmental Panel on Climate Change*; Solomon, S., Qin, D., Manning, M., Chen, Z., Marquis, M., Averyt, K.B., Tignor, M., Miller, H.L., Eds.; Cambridge University Press: Cambridge, UK, 2007; pp. 747–846.

22. Guppy, M.; Withers, P. Metabolic depression in animals: physiological perspectives and biochemical generalizations. *Biol. Rev.* **1999**, *74*, 1–40.

23. Pörtner, H.O. Climate-dependent evolution of Antarctic ectotherms: an integrative analysis. *Deep-Sea Res. II* **2006b**, *53*, 1071–1104.

24. Sommer, A.; Klein, B.; Pörtner, H.O. Temperature induced anaerobiosis in two populations of the polychaete worm *Arenicola marina*. *J. Comp. Physiol. B* **1997**, *16*, 725–735.

25. van Dijk, P.L.M.; Tesch, C.; Hardewig, I.; Pörtner, H.O. Physiological disturbances at critically high temperatures. A comparison between stenothermal Antarctic and eurythermal temperate eelpouts (Zoarcidae). *J. Exp. Biol.* **1999**, *202*, 3611–3621.

26. Abele, D.; Puntarulo, S. Formation of reactive species and induction of antioxidant defence systems in polar and temperate marine invertebrates and fish. *Comp. Physiol. Ecol. Part A* **2004**, *138*, 405–415.

27. Lannig, G.; Bock, C.; Sartoris, F.J.; Pörtner, H.O. Oxygen limitation of thermal tolerance in cod, *Gadus morhua* L. studied by magnetic resonance imaging and on-line venous oxygen monitoring. *Am. J. Physiol.* **2004**, *287*, R902–R910.

28. Wittmann, A.C.; Schröer, M.; Bock, C.; Steeger, H.U.; Paul, R.J.; Pörtner, H.O. Indicators of oxygen- and capacity limited thermal tolerance in the lugworm *Arenicola marina. Clim. Res.* **2008**, *37*, 227–240.

29. Pörtner, H.O.; Lannig, G. Oxygen and Capacity limited Thermal Tolerance. In *Fish Physiology: Hypoxia*; Richards, J.G., Farrell, A.P., Brauner, C.J., Eds.; London Academic: London, UK, 2009; Volume 27, pp.143–191.

30. Metzger, R.; Sartoris, F.J.; Langenbuch, M.; Pörtner, H.O. Influence of elevated CO_2 concentrations on thermal tolerance of the edible crab *Cancer pagurus. J. Thermal. Biol.* **2007**, *32* (3), 144–151.

31. Walther, K.; Sartoris, F.J.; Bock, C.; Pörtner, H.O. Impact of anthropogenic ocean acidification on thermal tolerance of the spider crab *Hyas araneus. Biogeosci. Discuss.* **2007**, *6*, 2837–2861.

32. Michaelidis, B.; Ouzounis, C.; Paleras, A.; Pörtner, H.O. Effects of long-term moderate hypercapnia on acid-base balance and growth rate in marine mussels *Mytilus galloprovincialis. Mar. Ecol. Prog. Ser.* **2005**, *293*, 109–118.

33. Pörtner, H.O. Ecosystem effects of ocean acidification in times of ocean warming: a physiologist's view. *Mar. Ecol. Prog. Ser.* **2008**, *373*, 203–217.

34. Shirayama, Y.; Thornton, H. Effect of increased atmospheric CO_2 on shallow water marine benthos. *J. Geophys. Res.* **2005**, *110*, C09S08, doi:10.1029/2004JC003618.

35. Pörtner, H.O.; Langenbuch, M.; Michaelidis, B. Synergistic effects of temperature extremes, hypoxia and increases in CO_2 on marine animals: from earth history to global change. *J. Geophys. Res.* **2005**, *110*, C09S10, doi:10.1029/2004JC002561.

36. Seibel, B.A.; Fabry, V.J. Marine biotic response to elevated carbon dioxide. *Adv. Appl. Biodiv. Sci.* **2003**, *4*, 59–67.

37. Lindinger, M.I.; Lawren, D.J.; McDonald, D.G. Acid–base balance in the sea mussel *Mytilus edulis*. Effects of environmental hypercapnia on intra and extracellular acid–base balance. *Mar. Biol. Lett.* **1984**, *5*, 371–381.

38. Nienhuis, S.; Palmer, A.R.; Harley, C.D.G. Elevated CO_2 affects shell dissolution rate but not calcification rate in a marine snail. *Proc. R. Soc. B* **2010**, doi:10.1098/rspb.2010.0206.

39. DeFur, P.L.; McMahon, B.R. Physiological compensation to short term air exposure in red rock crabs *Cancer productus* from littoral and sublittoral habitats: Acid–base balance. *Physiol. Zool.* **1984**, *57*, 151–160.

40. Gazeau, F.; Quiblier, C.; Jansen, J.M,; Gattuso, J.P.; Middelburg, J.J.; Heip, C.H.R. Impact of elevated CO_2 on shellfish calcification. *Geophys. Res. Lett.* **2007**, *34*, L07603, doi:10.1029/2006GL028554.

41. Ries, J.B.; Cohen, A.L.; McCorkle, D.C. Marine calcifiers exhibit mixed responses to CO_2-induced ocean acidification. *Geol* **2009**, *37*, 1131–1134.

42. Berge, J.A.; Bierkeng, B.; Pettersen, O.; Schaanning, M.T.; Oxnevad, S. Effects of increased water concentrations of CO_2 on growth of the bivalve *Mytilus edulis* L. *Chemosphere* **2006**, *62*, 681–687.

43. Gutowska, M.A.; Pörtner, H.O.; Melzner, F. Growth and calcification in the cephalopod *Sepia officinalis* under elevated seawater pCO_2. *MEPS* **2008**, *373*, 303–309.

44. Fennel, K.; Wilkin, J.; Previdi, M.; Najjar, R. Denitrification effects on air-sea CO_2 flux in the coastal ocean: Simulations for the northwest North Atlantic. *Geophys. Res. Lett.* **2008**, *35*, L24608, doi:10.1029/2008GL036147.

45. Cao, L.; Caldeira, K. Atmospheric CO_2 stabilization and ocean acidification, *Geophys. Res. Lett.* **2008**, *35*, L19609, doi:10.1029/2008GL035072.

46. Turley, C.; Eby, M.; Ridgwell, A.J.; Schmidt, D.N.; Findlay, H.S.; Brownlee, C.; Riebesell, U.; Fabry, V.J.; Feely, R.A.; Gattuso, J.P. The societal challenge of ocean acidification. *Mar. Poll. Bull.* **2010**, *60*, 787–792.

47. Brewer, P.G.; Bradshow, A.L.; Williams, R.T. Measurement of total carbon dioxide and alkalinity in the North Atlantic Ocean in 1981. In *The Changing Carbon Cycle—A Global Analysis*; Trabalka, J.R., Reichle, D.E., Eds.; Springer: New York, NY, USA, 1986; pp. 358–381.

48. Lewis, E.; Wallace, D. *Program Development for CO₂ System Calculations*; Carbon Dioxide Information Analysis Center, Oak Ridge National Laboratory: Oak Ridge, TN, USA, 1998.

49. Mehrbach, C.; Culberson, C.; Hawley, J.; Pytkovicz, R. Measurement of the apparent dissociation constants of carbonic acid in seawater at atmospheric pressure. *Limnol. Oceanogr.* **1973**, *18*, 897–907.

50. Dickson, A.G.; Millero, F.J. A comparison of the equilibrium constants for the dissociation of carbonic acid in seawater media. *Deep-Sea Res*. **1987**, *34*, 1733–1743.

51. Gutowska, M.A.; Melzner, F.; Pörtner, H.O.; Meier, S. Cuttlebone calcification increases during exposure to elevated seawater pCO_2 in the cephalopod *Sepia officinalis*. *Mar. Biol.* **2010**, *157*, 1653–1663.

52. Trimborn, S.; Wolf-Gladrow, D.; Richter, K.U.; Rost, B. The effect of pCO_2 on carbon acquisition and intracellular assimilation in four marine diatoms. *J. Exp. Mar. Biol. Ecol.* **2009**, *376*, 26–36.

53. Pörtner, H.O.; Boutilier, R.G.; Tang, Y.; Toews, D.P. Determination of intracellular pH and PCO_2 after metabolic inhibition by fluoride and nitrilotriacetic acid. *Respir. Physiol.* **1990**, *81*, 255–274.

54. Heisler, N. Buffering and transmembrane ion transfer processes. In *Acid-Base Regulation in Animals*; Heisler, N., Ed.; Elsevier: Amsterdam, The Netherlands, 1986; pp. 3–47.

55. Wittmann, A.C.; Held, C.; Pörtner, H.O.; Sartoris, F.J. Ion regulatory capacity and the biogeography of Crustacea at high southern latitudes. *Polar Biol.* **2010**, *33*, 919–928.

56. Lynch, M.J.; Master, J.; Pryor, J.P.; Lindon, J.C.; Spraul, M.; Foxall, P.J.D.; Nicholson, J.K. Ultra high field NMR spectroscopic studies on human seminal fluid, seminal vesicle and prostatic secretions. *J. Pharm. Biomed. Anal.* **1994**, *12*, 5–19.

57. Willker, W.; Engelmann, J.; Brand, A.; Leibfritz, D. Metabolite identification in cell extracts and culture media by proton-detected 2D-H,C-NMR spectroscopy. *J. Magn. Reson. Anal.* **1997**, *2*, 21–32.

58. Viant, M.R.; Rosenblum, E.S.; Tjeerdema, R.S. NMR based metabolomics: A powerful approach for characterizing the effects of environmental stressors on organism health. *Environ. Sci. Technol.* **2003**, *37*, 4982–4498.

59. Pinero-Sagredo, E.; Nunes, S.; Jose, M.; de los Santos, J.; Celda, B.; Esteve, V. NMR metabolic profile of human follicular fluid. *NMR Biomed.* **2010**, *23*, 485–495.

60. Bubb, W.A.; Wright, L.C.; Cagney, M.; Santangelo, R.T.; Sorrell, T.C.; Kuchel, P.W. Heteronuclear NMR studies of metabolites produced by *Cryptococcus neoformans* in culture media: identification of possible virulence factors. *Magn. Reson. Med.* **1999**, *42*, 442–453.

61. Sze, D.Y.; Jardetzky, O. Determination of metabolite and nucleotide concentrations in proliferating lymphocytes by ^{1}H NMR of acid extracts. *Biochim. Biophys. Acta* **1990**, *1054*, 181–197.

62. Dabos, K.J.; Parkinson, J.A.; Hewage, C.; Nelson, L.J.; Sadler, I.H.; Hayes, P.C.; Plevris, J.N. ^{1}H NMR spectroscopy as a tool to evaluate key metabolic functions of primary porcine hepatocytes after cryopreservation. *NMR Biomed.* **2002**, *15*, 241–250.

63. Lannig, G.; Flores, F.J.; Sokolova, I.M. Temperature-dependent stress response in oysters, *Crassostrea virginica*: Pollution reduces temperature tolerance in oysters. *Aquat. Toxicol.* **2006**, *79*, 278–287.

64. Bougrier, S.; Geairon, P.; Deslous-Paoli, J.M.; Bacher, C.; Jonquieres, G. Allometric relationships and effects of temperature on clearance and oxygen consumption rates of *Crassostrea gigas* (Thunberg). *Aquaculture* **1995**, *134*, 143–154.

65. Lucas, A.P.; Beninger, G. The use of physiological condition index in marine bivalve aquaculture. *Aquaculture* **1985**, *44*, 187–200.

66. Cruz-Rodriguez, L.A.; Baucum, A.J.; Soudant, P.; Chu, F.-L.E.; Hale, R.C. Effects of PCBs sorbed to algal paste and sediments on stress protein response (HSP70 family) in the eastern oyster, *Crassostrea virginica. Mar. Environ. Res.* **2000**, *50*, 341–345.

67. Cherkasov, A.S.; Biswas, P.K.; Ridings, D.M.; Ringwood, A.H., Sokolova, I.M. Effects of acclimation temperature and cadmium exposure on cellular energy budgets in the marine mollusk *Crassostrea virginica*: linking cellular and mitochondrial responses. *J. Exp. Biol.* **2006**, *209*, 1274–1284.

68. Reipschläger, A.; Pörtner, H.O. Metabolic depression during environmental stress: The role of extracellular versus intracellular pH in *Sipunculus nudus. J. Exp. Biol.* **1996**, *199*, 1801–1807.

69. Willson, L.L.; Burnett, L.E. Whole animal and gill tissue oxygen uptake in the Eastern oyster, *Crassostrea virginica*: Effect of hypoxia, hypercapnia, air exposure, and infection with the protozoan parasite *Perkinsus marinus*. *J. Exp. Mar. Biol. Ecol.* **2000**, *246*, 223–240.

70. Krumschnabel, G.; Schwarzbaum, P.J.; Wieser, W. Coupling of energy supply and energy demand in isolated goldfish Hepatocytes. *Physiol. Zool.* **1994**, *67*, 438–448.

71. Mark, F.C.; Hirse, T.; Pörtner, H.O. Thermal sensitivity of cellular energy budgets in some Antarctic fish hepatocytes. *Polar Biol.* **2005**, *28*, 805–814.

72. Addadi, L.; Joester, D.; Nudelman, F.; Weiner, S. Mollusk Shell Formation: A Source of New Concepts for Understanding Biomineralization Processes. *Chem. Eur. J*. **2006**, *12*, 980–987.

73. Palmer, A.R. Relative cost of producing skeletal organic matrix versus calcification: evidence from marine gastropods. *Mar. Biol*. **1983**, *75*, 287–292.

74. Palmer, A.R. Calcification in Marine Molluscs: How Costly is it? *Proc. Natl. Acad. Sci.* **1992**, *89*, 1379–1382.

75. Digby, P.S.B. The mechanism of calcification in the molluscan shell. In *Symposium of Zoological Society of London. Studies in the Structure*, *Physiology and Ecology of Molluscs*; Fretter, V., Ed.; Academic Press: London, UK, 1968; pp. 93–107.

76. Wheeler, A.P. Mechanisms of molluscan shell formation. In *Calcification in Biological Systems*; Bonucci, E., Ed.; CRC Press: Boca Raton, FL, USA, 1992.

77. Mount, A.S.; Wheeler, A.P.; Paradkar, R.P.; Snider, D. Hemocyte-mediated shell mineralization in the eastern oyster. *Science* **2004**, *304*, 297–300.

78. Day, E.G.; Branch, G.M.; Viljoen, C. How costly is molluscan shell erosion? A comparison of two patellid limpets with contrasting shell structures. *J. Exp. Mar. Biol. Ecol.* **2000**, *243*, 185–208.

79. Kurihara, H.; Asai, T.; Kato, S.; Ishimatsu, A. Effects of elevated p CO_2 on early development in the mussel *Mytilus galloprovincialis*. *Aquat. Biol.* **2008**, *4*, 225–233.

80. Wood, H.; Spicer, J.I.; Widdicombe, S. Ocean acidification may increase calcification rates, but at a cost. *Proc. R. Soc. B* **2008**, *275*, 1767–1773.

81. Thomsen, J.; Melzner, F. Seawater acidification does not elicit metabolic depression in the blue mussel *Mytilus edulis*. *Mar. Biol.* **2010**, Submitted.

82. Langenbuch, M.; Pörtner, H.O. Energy budget of hepatocytes from Antarctic fish (Pachycara brachycephalum and Lepidonotothen kempi) as a function of ambient CO_2: pH-dependent limitations of cellular protein biosynthesis? *J. Exp. Biol.* **2003**, *206*, 3895–3903.

83. Langenbuch, M.; Bock, C.; Leibfritz, D.; Pörtner, H.O. Effects of environmental hypercapnia on animal physiology: A ^{13}C NMR study of protein synthesis rates in the marine invertebrate *Sipunculus nudus*. *Comp. Biochem. Physiol. A* **2006**, *144*, 479–484.

84. Grieshaber, M.K.; Hardewig, I.; Kreutzer, U.; Poertner, H.O. Physiological and metabolic responses to hypoxia in invertebrates. *Rev. Physiol. Biochem. Pharmacol*. **1994**, *125*, 143–147.

85. Kurochkin, I.O.; Ivanina, A.V.; Eilers, S.; Downs, C.A.; May, L.A.; Sokolova, I.M. Cadmium affects metabolic responses to prolonged anoxia and reoxygenation in eastern oysters *Crassostrea virginica*. *Am. J. Physiol.* **2009**, R1262–R1272.

86. Michaelidis, B.; Haas, D.; Grieshaber, M.K. Extracellular and Intracellular Acid-Base Status with Regard to the Energy Metabolism in the Oyster *Crassostrea gigas* during Exposure to Air. *Physiol. Biochem. Zool.* **2005**, *78*, 373–383.

87. Deigweiher, K. Impact of high CO_2 concentrations on marine life: Molecular mechanisms and physiological adaptations of pH and ion regulation in marine fish. PhD Thesis, University of Bremen, Bremen, Germany, 2009.

88. Thomsen, J.; Gutowska, M.A.; Saphörster, J.; Heinemann, A.; Trübenbach, K.; Fietzke, J.; Hiebenthal, C.; Eisenhauer, A.; Körtzinger, A.; Wahl, M.; Melzner, F. Calcifying invertebrates succeed in a naturally CO_2 enriched coastal habitat but are threatened by high levels of future ocean acidification. *Biogeosci. Dis.* **2010**, *7*, 5119–5156, doi:10.5194/bgd-7-5119-2010.

89. Zittier, Z.M.C.; Kutsch, B.; Bock, C.; Pörtner, H.O. Synergistic impacts of ocean acidification and temperature increase on the physiology of *Mytilus edulis*. Presented at the *Annual Main Meeting of Society for Experimental Biology (SEB), C8: General Thermal Biology*, Prague, Czech Republic, June/July 2010.

90. Stark, A.; Treydte, T.; Heilmeyer, O.; Brey, T.; Pörtner, H.O. Is the Greenland smoothcockle (*Serripes groenlandicus*) sensitive to elevated CO_2 and temperature levels? Presented at the *Annual Main Meeting of Society for Experimental Biology (SEB), C1: Polar adaptations & challenges*, Prague, Czech Republic, June/July 2010.

91. Hardewig, I.; Pörtner, H.O.; Grieshaber, M.K. Interactions of anaerobic propionate formation and acid-base status in *Arenicola marina*: an analysis of propionyl-CoA carboxylase. *Physiol. Zool.* **1994**, *67*, 892–909.

92. Pörtner, H.O. Contributions of anaerobic metabolism to pH regulation in animal tissues: theory. *J. Exp. Biol.* **1987**, *131*, 69–87.

93. Pörtner, H.O.; Bock, C.; Reipschläger, A. Modulation of the cost of pH_i regulation during metabolic depression: a ^{31}P-NMR study in invertebrate (*Sipunculus nudus*) isolated muscle. *J. Exp. Biol.* **2000**, *203*, 2417–2428.

94. Seidelin, M.; Brauner, C.J.; Jensen, F.B.; Madsen, S.S. Vacuolar-type H+-ATPase and Na+, K+-ATPase expression in gills of Atlantic salmon (*Salmo salar*) during isolated and combined exposure to hyperoxia and hypercapnia in fresh water. *Zoolog. Sci.* **2001**, *18* (9), 1199–1205.

95. Deigweiher, K.; Koschnick, N.; Pörtner, H.O.; Lucassen, M. Acclimation of ion regulatory capacities in gills of marine fish under environmental hypercapnia. *Am. J. Physiol.* **2008**, *295*, R1660–R1670.

96. Pörtner, H.O.; Bock, C. A contribution of acid-base regulation to metabolic depression in marine ectotherms. In *Life in the Cold*; Heldmaier, G., Klingenspor, M., Eds.; Springer Verlag: Berlin, Germany, 2000; pp. 443–458.

97. Marshall, W.S. Na+, Cl-, Ca2+ and Zn2+ transport by fish gills: retrospective review and prospective synthesis. *J. Exp. Zool.* **2002**, *293* (3), 264–283.

98. Perry, S.F.; Gilmour, K.M. Acid-base balance and CO_2 excretion in fish: unanswered questions and emerging models. *Respir. Physiol. Neurobiol.* **2006**, *154* (1–2), 199–215.

99. Parker, L.M.; Ross, P.M.; O'Connor, W.A. The effect of ocean acidification and temperature on the fertilization and embryonic development of the Sydney rock oyster *Saccostrea glomerata* (Gould 1850). *Global Change Biol.* **2009**, *15*, 2123–2136.

100. Sokolova, I.M.; Lannig, G. Interactive effects of metal pollution and temperature on metabolism in aquatic ectotherms: Implications of global climate change. *Clim. Res.* **2008**, *37*, 181–201.